J Intell Robot Syst (2014) 75:71–86
DOI 10.1007/s10846-013-9868-9

A Simplified CPGs Network with Phase Oscillator Model for Locomotion Control of a Snake-like Robot

Norzalilah Mohamad Nor · Shugen Ma

Received: 19 February 2013 / Accepted: 17 July 2013 / Published online: 8 August 2013

Abstract CPG (Central pattern generator) is a dynamical system of coupled nonlinear oscillators or neural networks inspired by a control mechanism in animal bodies. Without any rhythmic inputs, the CPG has the ability to produce oscillatory patterns. This paper presents a novel structure of a CPG network which can produce rhythmic motion that imitates movement of animals such as snake and lamprey. The focus is on the locomotion control of a snake-like robot, where phase oscillator has been adopted as the dynamical model to control the harmonic motion of the CPG network. There are two main points addressed in this paper: (1) simple network structure of unidirectional coupling oscillators, and (2) a single parameter to control the body shape and to control the forward and backward movement of the snake-like robot. The proposed CPG network is designed to have a simple structure with less complexity, less mathematical computation, fast convergence speed and exhibit limit cycle behavior. In addition, a new parameter, τ is introduced to control the smoothness of the CPG output as well as the speed of the snake-like robot. Simulation and experimental results show that the proposed CPG network can be used to control the serpentine locomotion of a snake-like robot.

Keywords Central pattern generator · Phase oscillator · Snake-like robot

N. M. Nor · S. Ma (✉)
Department of Robotics, Ritsumeikan University, Kusatsu, Shiga, Japan
e-mail: shugen@se.ritsumei.ac.jp

N. M. Nor
e-mail: gr0119hx@ed.ritsumei.ac.jp

1 Introduction

Central pattern generator or CPG is a neural network that exists in spinal cords of living animals which is used as activation signal for muscle contractions in animals. Without any rhythmic inputs from sensory feedback or from higher control centers, the CPG can produce coordinated patterns or rhythmic activity [1]. The bionic control process is shown in Fig. 1.

By applying CPG concept as the control mechanism of some biological robots, we can imitate the rhythmic locomotion such as walking, crawling and swimming. From control point of view, the control architecture of biological robots can be categorized into three architectures: (i) sine based, (ii) model based, and (iii) CPG-based. The first two categories are the conventional methods, while the CPG-based is the alternative method that use dynamical systems of coupled nonlinear oscillators. The advantages of CPG-based approaches are due to their low computational cost,

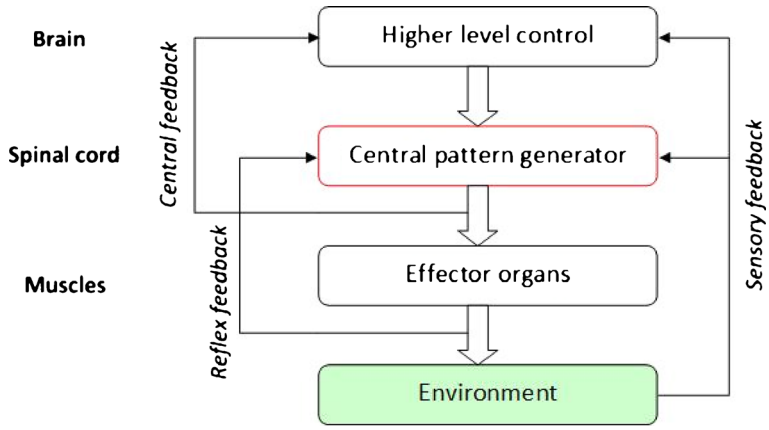

Fig. 1 Bionic control process [1]

exhibits limit cycle behavior and parameters that have clear relationship with the output. Further reading on the comparisons between these three control architecture can be found in [2].

This paper contains some parts of Nor's [3] work which focus on the locomotion control using CPG network for a snake-like robot. It is known that natural snakes can perform various locomotion shapes depending on its surrounding where its locomotion can be classified into four categories namely serpentine, sidewinding, rectilinear and concertina. The typical locomotion of snakes is the serpentine locomotion, which can be described as S-shape movement [1, 2, 4, 5]. For serpentine mode, each part of the snake body makes similar tracks, which is the most efficient among all modes [5]. Therefore, the main focus of this paper is to mimic the S-shape movement of the natural snakes into our snake-like robot using our proposed CPG structure.

Based on the superiority of the natural snakes movement, many researchers have developed snake-like robots with various control designs. Most of researchers focus on controlling the locomotion of moving forward and/or backward of mobile robots with rhythmic movement patterns using CPG-based control. Zhou and Low [6] designed locomotion control of a fish robot with fin propulsion. The CPG-based control method illustrates a way to switch motion patterns by simply tuning corresponding parameters. But, their CPG network is not suitable to control locomotion of a snake-like robot. Crespi and Ijspeert [7] utilized CPG-locomotion control for online optimization of amphibious snake robot. They utilize bidirectional CPG coupling which complicates the CPG structure. Lu et al. [8] analyzed snake-like robot controlled by cyclic inhibitory CPG model where all the parameters of the CPG are fixed during the locomotion. Wu [9] improved the CPG connection model and analyzed the effect of CPG parameters to the CPG output without changing any parameters at any time instance. Tang and Ma [10] proposed a self-tuning multi phase CPG which enables the snake-like robot to adapt to environments. All of these papers have either of the drawbacks: (1) complicated CPG networks, (2) high computational cost, and (3) complex interneurons connection to produce rhythmic output.

To overcome all the above mentioned drawbacks, a novel CPG network so-called unidirectional coupling oscillator with simple structure is proposed. Phase oscillator is adopted as the dynamic model representing our CPG coupled oscillators. There are other types of oscillators such as van der Pol, Stein, FitzHugh-Nagumo [11], Matsuoka oscillators [9] and Hopf oscillator [6, 12]. All of the mentioned oscillators have its own drawbacks. For instance, the mathematical model of the Matsuoka oscillators provides several parameters that influence the CPG output. Some of the parameters are interrelated to each other and need to follow some numerical conditions [9]. It makes the robot's control become complicated and difficult. Meanwhile, for Hopf oscillator, the coupling terms between oscillators need to be further derived from the nonlinear differential equation [6]. In contrast, the phase

oscillator model resembles the sine-based function in terms of its parameters relationship to the output. The frequency, phase, and amplitude are directly influenced the CPG output, which provides easy control. The phase oscillator model possesses attractive characteristics such as: limit cycle and robust. The advantage of using CPG-based model over the sine-based is that it offers the possibility to integrate sensory feedback signals in the differential equation [13, 14]. Further reading on various applications of CPG can be referred to [17–30].

The proposed unidirectional coupling oscillator provides simple coupling with each CPG oscillators, less mathematical computation, fast convergence speed and less complexity. First, we will compare our proposed CPG structure with the bidirectional CPG structure [7] and show the uniqueness of our CPG structure in producing homogeneous output waves. Also, the stability of our CPG structure, relation between parameters and effects of each parameter to the output will be analyzed in detail.

This paper is organized as follows: Section 2 describes the structure of CPG model for generating rhythmic motion, Section 3 presents the analysis of unidirectional coupling oscillators, Section 4 presents the implementation to a snake-like robot, Section 5 shows the simulation results, Section 6 presents the experimental results of the proposed CPG network, Section 7 is the discussion of overall results and finally Section 8 is the concluding remarks as well as our future works.

2 CPG Model for Generating Rhythmic Motion

This section describes the mathematical model and structure of our proposed CPG model. Furthermore, we analyze our proposed CPG structure with bidirectional structure proposed by Crespi and Ijspeert [7] in terms of coupling complexity, mathematical computation and convergence speed to phase locking state.

2.1 Mathematical Model

Nonlinear model of phase oscillator has been utilized to control locomotion of amphibious snake robot and modular robot [7, 15]. The mathematical model describing a system of one phase oscillator is as follows:

$$\dot{\theta}_i = 2\pi v_i + \sum w_{ij} \sin(\theta_j - \theta_i) \tag{1}$$

Detail explanations of the parameters in Eq. 1 can be referred in Table 1. This oscillator model spontaneously produces traveling waves with constant phase difference between neighboring segments along the body, and it is made of multiple oscillators connected as a double chain, and Eq. 1 has been modified [7] as follows:

$$\dot{\theta}_i = 2\pi v_i + \sum w_{ij} \sin(\theta_j - \theta_i - \phi_{ij}) \tag{2}$$

where ϕ_{ij} is the phase bias. Here, ϕ_{ij} is used to determine the phase lag between oscillators. Coupling term between the oscillators is defined by the weights w_{ij} and the phase bias ϕ_{ij}. The output for each oscillator is as follows:

$$x_i = A \cos(\theta_i) \tag{3}$$

Description of parameters in Eqs. 2 and 3 are shown in Table 1.

2.2 Structure of CPG Models

For the phase oscillator model, bidirectional coupling is usually adopted to control one actuator. Figure 2a illustrates the structure of multiple phase oscillator connected as a double chain. This type of coupling structure has been implemented by Crespi and Ijspeert [7]. Figure 2b shows our proposed CPG structure using the phase oscillator model, which is unidirectional coupling. Referring to Fig. 2b, for simplicity, we named these oscillators from left to right as: oscillator 1, oscillator 2, oscillator 3 and so on in ascending order.

Table 1 Description of the parameters

Items	Details
θ_i	Phase of the ith oscillator
θ_j	Phase of the jth oscillator
v_i	Intrinsic frequency
A	Amplitude
w_{ij}	Coupling weights between oscillators
ϕ_{ij}	Phase bias
x_i	Rhythmic and positive output signal
$\dot{\theta}_i$	The time evolution of the phase θ_i

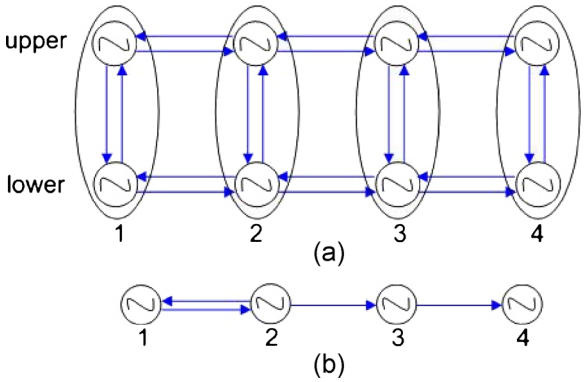

Fig. 2 Structure of coupling oscillator: **a** bidirectional coupling, and **b** unidirectional coupling

Referring to Fig. 2, the direction of arrow for each oscillator indicates the receiving θ_j (inward) from neighbor oscillator or transmitting θ_i (outward) to neighbor oscillator.

For bidirectional coupling, two neurons are adopted to control one output signal. For simplicity, we named the upper part as *[u]*, and the lower part as *[l]*. The mathematical model used to describe θ_i as in Fig. 2a for $i = 1, 2, 3$ is as follows:

$$\dot{\theta}_{1[l]} = 2\pi\nu_{1[l]} + w_{1[l]2[l]}\sin(\theta_{2[l]} - \theta_{1[l]} + \phi_{1[l]2[l]}) + w_{1[l]1[u]}\sin(\theta_{1[u]} - \theta_{1[l]} - \phi_{1[l]1[u]}) \quad (4)$$

$$\dot{\theta}_{2[l]} = 2\pi\nu_{2[l]} + w_{2[l]1[l]}\sin(\theta_{1[l]} - \theta_{2[l]} - \phi_{2[l]1[l]}) + w_{2[l]3[l]}\sin(\theta_{3[l]} - \theta_{2[l]} + \phi_{2[l]3[l]}) + w_{2[l]2[u]}\sin(\theta_{2[u]} - \theta_{2[l]} - \phi_{2[l]2[u]}) \quad (5)$$

$$\dot{\theta}_{3[l]} = 2\pi\nu_{3[l]} + w_{3[l]2[l]}\sin(\theta_{2[l]} - \theta_{3[l]} - \phi_{3[l]2[l]}) + w_{3[l]4[l]}\sin(\theta_{4[l]} - \theta_{3[l]} + \phi_{3[l]4[l]}) + w_{3[l]3[u]}\sin(\theta_{3[u]} - \theta_{3[l]} - \phi_{3[l]3[u]}) \quad (6)$$

For simplicity but without loss of generality, the value of ϕ_{ij} can be respectively assigned to ϕ for descending connections and $-\phi$ for ascending connection. For upper and lower connections, the value of ϕ_{ij} is set to $-\phi$ for downward connections, and ϕ for upward connections. The CPG network proposed in [7] is structurally complicated and difficult to analyze numerically. Besides, it is not easy to change the phase difference because of the strong coupling between the oscillators. Furthermore, the number of connections in bidirectional network as in Fig. 2a is three times more than our network which increases the calculation time significantly. Due to the said drawbacks, we propose simple CPG coupling so-called unidirectional coupling for a snake-like robot locomotion control. As shown in Fig. 2b, only one neuron is adopted for controlling one output signal, and the mathematical model used to describe θ_i for $i = 1, 2, 3$ is as follows:

$$\dot{\theta}_1 = 2\pi\nu_1 + w_{12}\sin(\theta_2 - \theta_1 - \phi_{12}) \quad (7)$$

$$\dot{\theta}_2 = 2\pi\nu_2 + w_{21}\sin(\theta_1 - \theta_2 + \phi_{21}) \quad (8)$$

$$\dot{\theta}_3 = 2\pi\nu_3 + w_{32}\sin(\theta_2 - \theta_3 + \phi_{32}) \quad (9)$$

The design of our CPG network is rather simple in structure by connecting it into unidirectional CPGs network (see Fig. 2b). In this model, the oscillators are connected in a direction from head to the tail of the snake-like robot. Referring to Fig. 2b, the first two oscillators are coupled bidirectionally because every phase oscillator needs to have input from other CPG in order to produce harmonic rhythmic output. The value of ϕ_{ij} is set to ϕ for descending connections and $-\phi$ for ascending connection. The desired joint angles for unidirectional coupling are described as:

$$joint\_angle[i] = x_i \quad (10)$$

The behavior of θ_i and desired joint angles of the unidirectional CPGs network are shown in Fig. 3. The parameters used are: $\nu_i = 0.1$, $w_{ij} = 10$, $A = 1$, and $\phi = \pm\pi/3$ for all CPGs.

It is obvious that the output waves are homogeneously distributed with phase difference equal to ϕ. With unidirectional network, multi numbers of equations can be eliminated.

2.3 Convergence Speed to Phase Locking State

In previous subsection, we have already compared the complexity of the synapse connections between the two CPG models i.e., bidirectional and unidirectional structures. The results conclude that the proposed unidirectional structure is superior over the bidirectional structure. In this subsection, we further analyze our proposed CPG model by comparing the two CPG models, based on the convergence speed to the phase locking

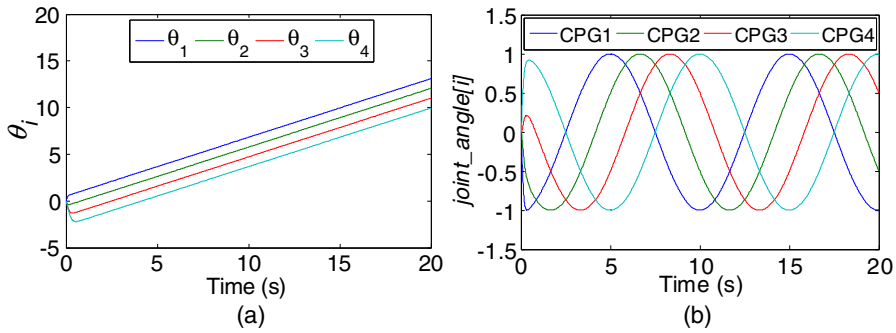

Fig. 3 Unidirectional CPG network: **a** behavior of θ_i, and **b** joint angle

state. We compared both the convergence speed of the unidirectional and bidirectional structure using the same CPU frequency and internal memory of 2.80 Ghz and 3.00 GB respectively with 64-bit operating system. The parameters used for both CPG models are: $w_{ij} = 10$, and $A = 1$. We simulate the results only for four CPG couplings and the interpretation of the CPGs is similar as in Fig. 3.

In Table 2, we show results of the convergence speed during the initial state to the phase locking state for the two CPG models. We analyze the convergence speed by varying the value of $v_i = 0.1$ and 1.0, and value of $\phi_{ij} = \pi/2, \pi/3$, and $\pi/6$.

From the results in Table 2, the convergence speed for bidirectional network is a bit faster than our proposed unidirectional coupling. But the difference of the convergence speed between these two models is only less than 0.5 s, which is small and acceptable while comparing with motion time. It thus can be disregarded.

Based on our analysis, the convergence speed does not depend on the value of v_i. There are two factors that affect the convergence speed for the initial state to be at the phase locking state: (1) the convergence speed increases as the number of oscillator increase, and (2) the convergence speed increases slightly as the value of ϕ_{ij} increase.

Table 2 Comparison of convergence speed

v_i	Convergence speed (s)		ϕ_{ij}
	Unidirectional	Bidirectional	
0.1	1.4	0.9	$\pi/2$
0.1	1.2	0.8	$\pi/3$
0.1	1.2	0.7	$\pi/6$
1.0	1.4	0.8	$\pi/2$
1.0	1.1	0.7	$\pi/3$
1.0	1.1	0.7	$\pi/6$

3 Analysis of CPG Model with Unidirectional Coupling

In this section, we will show that our proposed structure is much simpler and provides the same stability as the bidirectional coupling. The control of phase difference of the unidirectional oscillator will be proved to be easier rather than the bidirectional coupling. Some modifications also have been done in Eq. 2, to control the smoothness of the CPG outputs as well as to control the speed of the snake-like robot.

3.1 Descriptions of the Phase Oscillator Model

Firstly, for further understanding, we describe the similarity of the terms of the phase oscillator model with the conventional sine-based model used for controlling the rhythmic output wave, as shown in Table 3.

The sine-based uses simple time-indexed sine-based functions, while the CPG-based uses

Table 3 Similarity of the terms between sine-based and phase oscillator (CPG-based)

	Sine-based	CPG-based
Equation	$x_i = A \sin(\omega t + i\phi)$	$\dot{\theta}_i = 2\pi v_i + \sum w_{ij} \sin(\theta_j - \theta_i - \phi_{ij})$ $x_i = A\cos(\theta_i)$
Amplitude	A	A
Frequency	ω	$2\pi v_i$
Phase difference	ϕ	ϕ_{ij}
Output	x_i	x_i

dynamical systems of coupled nonlinear oscillators to generate traveling waves. Even though both control architectures have similar terms, but the drawbacks of the sine-based are [5]: (i) it is not efficient to modify its parameters online, and (ii) it is not easy to integrate sensory feedback signals. Thus, it is clear that the parameters of the phase oscillator model have clear relationship with the output. With this advantage, it is easy to control and adjust the parameters accordingly.

For our proposed CPG-based model, the parameters for v_i, w_{ij}, and ϕ_{ij} are set to have the same value for all of the CPG oscillators in controlling the locomotion of our snake-like robot. In other word, we define $v_i = v$, $w_{ij} = w$, and $\phi_{ij} = \phi$ for all oscillators.

3.2 Feedback Connection of the CPGs

In this section, we analyze the feedback connection of the oscillator 1. For our proposed CPG structure (Fig. 2b), the feedback connection is set from oscillator 2 to oscillator 1. With the set configuration, we can get homogeneous oscillations distribution between the oscillators output. The significant advantage of our proposed CPG structure with the feedback connection is that, the phase difference can be controlled by controlling parameter ϕ as shown in Fig. 3b. To further clarify the uniqueness of our CPG structure, we analyze the CPG outputs behavior when changing the feeding connection from other oscillators to oscillator 1. The parameters used are: $v = 1$, $w = 10$, and $A = 1$.

In Fig. 4, we show the behavior of the CPG output x_i in term of ϕ when we change the feedback connection to oscillator 1. The x-axis in Fig. 4 denotes oscillator 2, oscillator 3, and oscillator 4 while the y-axis denotes the value of ϕ with respect to the feedback connection. We analyze various values of ϕ (in degree) for $\phi = 90°$, $60°$, $45°$, and $30°$. From Fig. 4, we can conclude that there is a nonlinear changed in value of ϕ as the feedback connection varies increasingly with the sequence of oscillator. Therefore, the feedback connection must be fixed from oscillator 2 to oscillator 1 to get the desired phase difference based on the set value of ϕ.

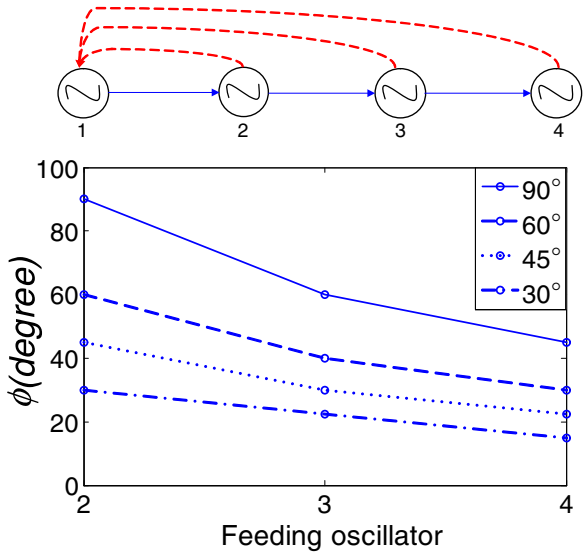

Fig. 4 Behavior of ϕ when the feedback connection is changed

We further analyze the changing of the sign of ϕ for oscillator 1. In our proposed CPG structure, the sign of the first oscillator (oscillator 1) must be reversed with other oscillators. In Fig. 5, we can see that the outputs x_i are in ascending order when ϕ for oscillator 1 is negative, whereas in Fig. 6, the outputs x_i are in descending order when ϕ for oscillator 1 is positive.

Based on our analysis, to produce homogeneous waves we can conclude the following:

(1) Oscillator 1 must always get feedback connection from oscillator 2;
(2) as the feedback connection varies increasingly with the sequence of oscillator, the value of ϕ change with nonlinear decreasing;
(3) the sign ($\pm$) for ϕ for oscillator 1 should always be opposite to the other oscillators;
(4) if sign of the ϕ for oscillator 1 is positive ($+$), the CPG outputs will be in descending order;
(5) if sign of the ϕ for oscillator 1 is negative ($-$), the CPG outputs will be in ascending order.

3.3 Phase Difference Synchronization

Stability analysis for two bidirectional coupled oscillator for determining synchronization of the phase difference can be referred to [7]. Also, more in depth analysis of networks of phase oscillators

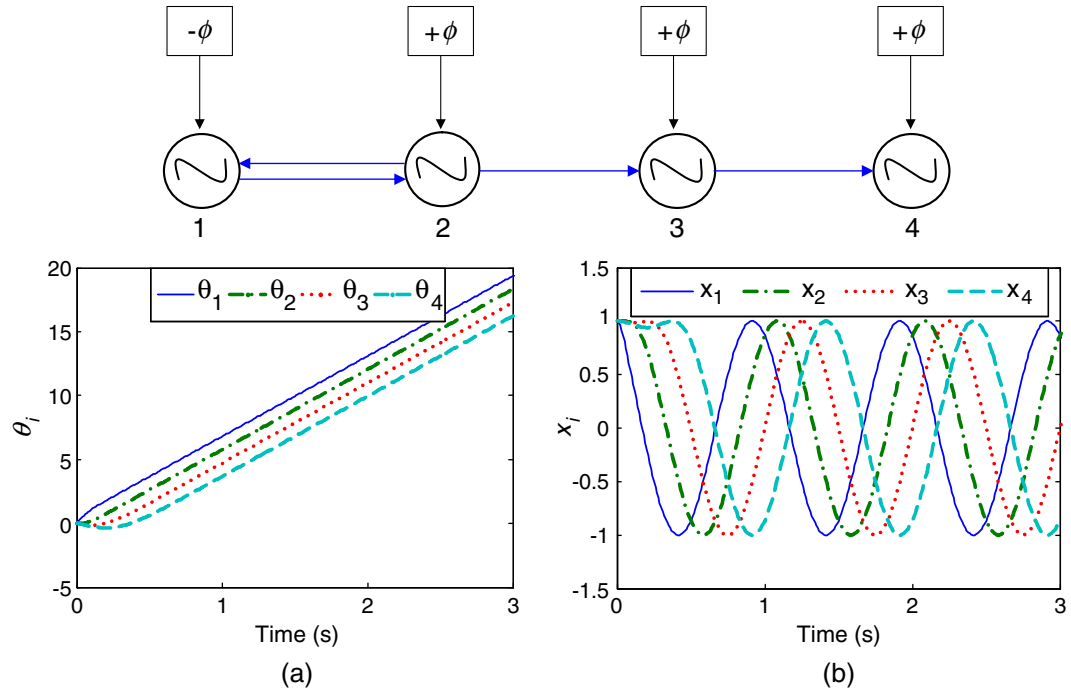

Fig. 5 Behavior of CPG when ϕ for oscillator 1 is negative $(-)$: **a** θ_i, and **b** output x_i

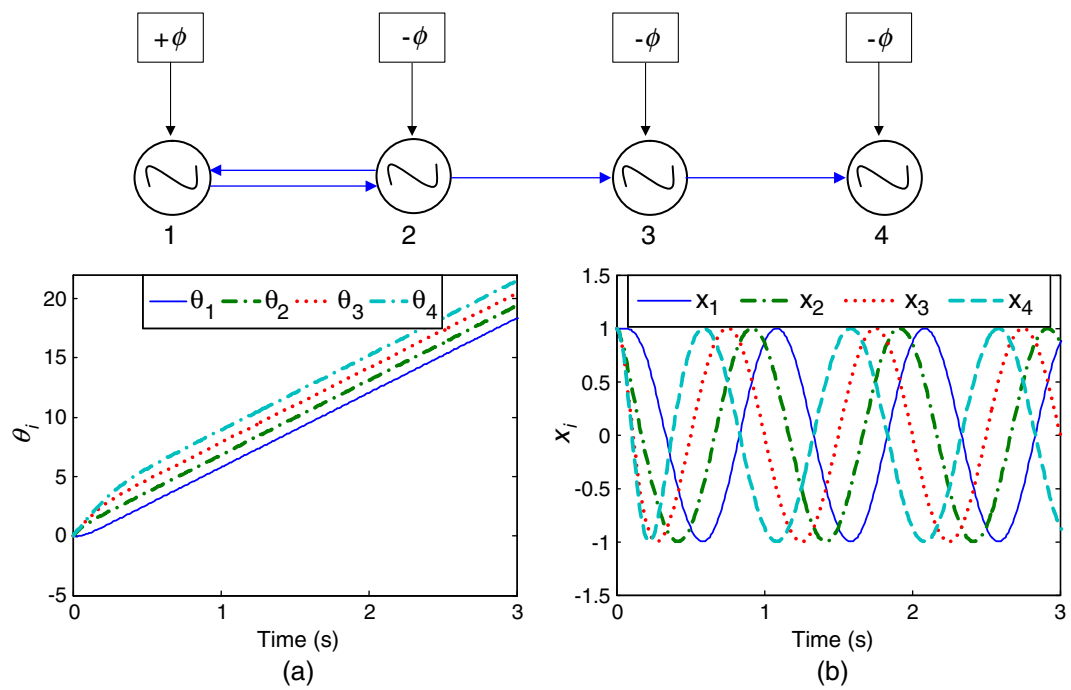

Fig. 6 Behavior of CPG when ϕ for oscillator 1 is positive $(+)$: **a** θ_i, and **b** output x_i

can be found in [15]. In this section, we are interested to determine whether the unidirectional coupled oscillators (Fig. 2b) will synchronize at constant phase difference.

The phase biases between the first two oscillators, oscillator 1 and oscillator 2 (refer Fig. 2b) must always be in opposite sign to obtain the rhythmic output with constant phase difference. For other oscillators i.e., oscillator 3, oscillator 4 and so on, the sign of ϕ must follow the sign of ϕ for oscillator 2. From Eq. 9, consider the case for oscillator 3:

$$f(\theta_3) = \dot{\theta}_3 = 2\pi v + w\sin(\theta_2 - \theta_3 + \phi) \tag{11}$$

For the first oscillator, we use $+\phi$ and $-\phi$ for other oscillators. The equilibrium occurs when the right hand sides of the first order system, Eq. 11, simultaneously vanishes [16]:

$$2\pi v + w\sin(\theta_2 - \theta_3 + \phi) = 0 \tag{12}$$

Solving Eq. 12 for θ_3, we obtain:

$$\theta_3^{\infty} = \theta_2 + \phi + \sin^{-1}(2\pi v/w) \tag{13}$$

From Eq. 13, we can see that θ_3 will always evolve at constant phase difference of $\theta_2 + \phi + \epsilon$, where $\epsilon = \sin^{-1}(2\pi v/w)$. In order to get the output of oscillator, x_i to converge to oscillations that are phase locked with a phase difference of ϕ, we must have:

$$v << w \tag{14}$$

So that ϵ will be relatively small and can be ignored. Therefore, the output will become: $x_3^{\infty}(t) = \cos(\theta_2 + \phi)$. Here, we can see that ϕ is a phase difference between θ_i and θ_{i-1}, where:

$$\theta_3 = \theta_2 + \phi \tag{15}$$

Therefore:

$$\begin{aligned}\phi &= \theta_3 - \theta_2 \\ &= \theta_i - \theta_{i-1} = \Delta\theta_i\end{aligned} \tag{16}$$

If rule in Eq. 14 is obeyed, the solution will be asymptotically stable because:

$$\left.\frac{\partial f(\theta_3)}{\partial \theta_3}\right|_{\theta_3^{\infty}} = -w\cos(\theta_2 - \theta_3 + \phi) \tag{17}$$

Substitute Eq. 13 into Eq. 17, we obtain:

$$\frac{\partial f(\theta_3^{\infty})}{\partial \theta_3} = -w\cos(\sin^{-1}(2\pi v/w)) \tag{18}$$

Equation 18 shows that the solution of $\partial f(\theta_3^{\infty})/\partial\theta_3 < 0$ at all value of ϕ. Note that Eq. 14 should be satisfied all times for every type of network connection because if value of $v \approx w$, the output wave will deteriorate.

3.4 Frequency Control

From the previous section, we can see that the output oscillator will evolve at constant phase difference $\pm\phi$. But, the effect of Eq. 14 to the output is that we need to control two parameters: v and w in order to produce smooth output. Parameter v can be used to control speed it determines the locomotion speed of the snake-like robot [7]. From our analysis by simulation, as we control the frequency, v, we need to adjust w as well. The

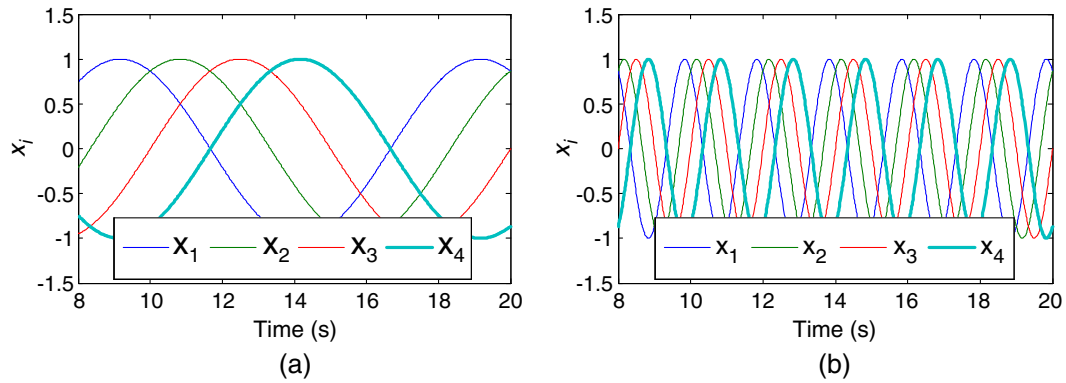

Fig. 7 Effect of variable τ to the output, **a** without τ, and **b** with $\tau = 0.2$

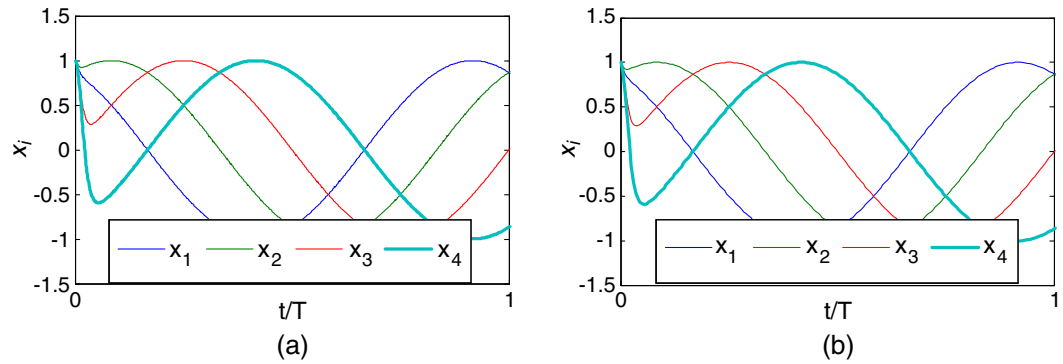

Fig. 8 Convergence rate to phase locking state, **a** without τ, and **b** with $\tau = 0.2$

CPG output will deteriorate if value of v is nearly to w, or if value of w is too large compared to v. To overcome this issue, we introduce a variable, τ as a single parameter to control both the frequency, v and weight, w of the oscillator. The modification of Eq. 2 is as follows:

$$\tau\dot{\theta}_i = 2\pi v + \sum w \sin(\theta_j - \theta_i - \phi) \tag{19}$$

The variable τ will not affect the phase locking of the output, where Eq. 13 can still be maintained even though we introduced a new variable in Eq. 19. Figure 7 shows the effect of using τ where Fig. 7a is the outputs without variable τ, and Fig. 7b is the outputs with variable τ. For easy view, we bold one of the CPGs output. From Fig. 7, we can see that by introducing variable τ, the requency of the output can be controlled without deteriorating the output or without needing to adjust the w, even the intrinsic frequency, v is small.

In Fig. 8, we also analyze whether τ gives any effects of convergence rate to phase locking state (i.e., stable state of the CPG output, x_i). Since the frequency is controlled by adjusting τ, we normalized the time by the output period, T in Fig. 7. We can see that the convergence rate is the same in both Fig. 8a and b, which is less than 0.1 s and thus, by introducing parameter τ, the convergence rate of the CPG output, x_i can still be maintained.

From Eq. 19, the value τ should be ≤ 1 to give effect to the output of CPG. If $\tau > 1$, the performance of the output will deteriorate.

3.5 Effects of Parameter τ to CPG Output Frequency

Figure 9 shows how the parameter τ affects the output frequency. The value of τ is 1, 1/5, 1/10, 1/15, and 1/20 with constant intrinsic frequency, $v = 0.1$ and $w = 10$. As the value of τ decreases, the output frequency will increase. But as τ gets smaller, the tendency for the output frequency to increase is slower. Referring to the line connecting between points in Fig. 9, we can see that the slope is getting smaller as τ decreases.

From Fig. 9, we can deduce that there is a limitation for adjusting the output frequency. The range of τ can be set from 1 to 1/15 to make the changes of frequency to be apparent. Also, if we set the value of τ to be much smaller, the output wave will tend to deteriorate. For application to a

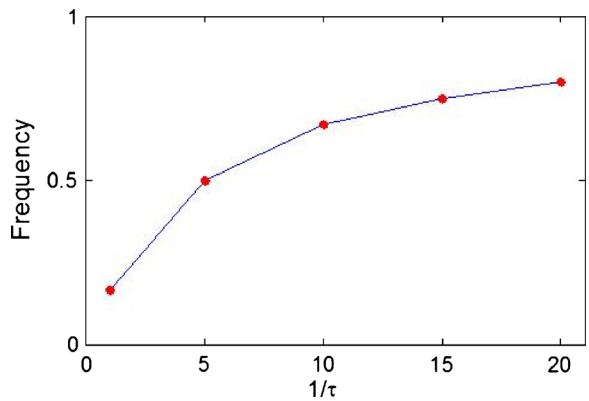

Fig. 9 Effect of τ to the output frequency

snake-like robot, the frequency can be used as a control parameter of the robot's speed.

3.6 Frequency Transition

One of the requirements of high performance locomotion control of robots is a smooth transition between different gaits. This is to avoid jerky or discontinuous locomotion which may damage the gear box or actuator of the robots. To prove the proposed CPG model can rapidly adapt to parameter change, we analyzed the reaction of the new parameter τ, by switching its value at random time instantly, whilst other CPG parameters are kept constant for all period of time.

Figure 10 shows the behavior of our CPG model when changing the value of parameter τ at random time of 25 and 40 s. From this figure, we can see that the output is stable during the transition. The output converges to the desired traveling wave after a short transient period. We can deduce that the CPG is adaptive to the change of parameter τ.

4 Implementation to a Snake-like Robot

Snake-like robot is one of an example of cord-shaped robot, which has large degree of freedoms. Many researches on controlling this kind of robot have been done based on interaction between mutually connected CPGs. For a snake-like robot, the phase difference should be adjusted continuously and must be easily controlled from head to tail.

Our CPG network can be implemented in a snake-like robot as shown in Fig. 11. One CPG will control one joint angle of the snake-like robot.

Due to the fact that the propelling force of the serpentine motion on a snake-like robot comes

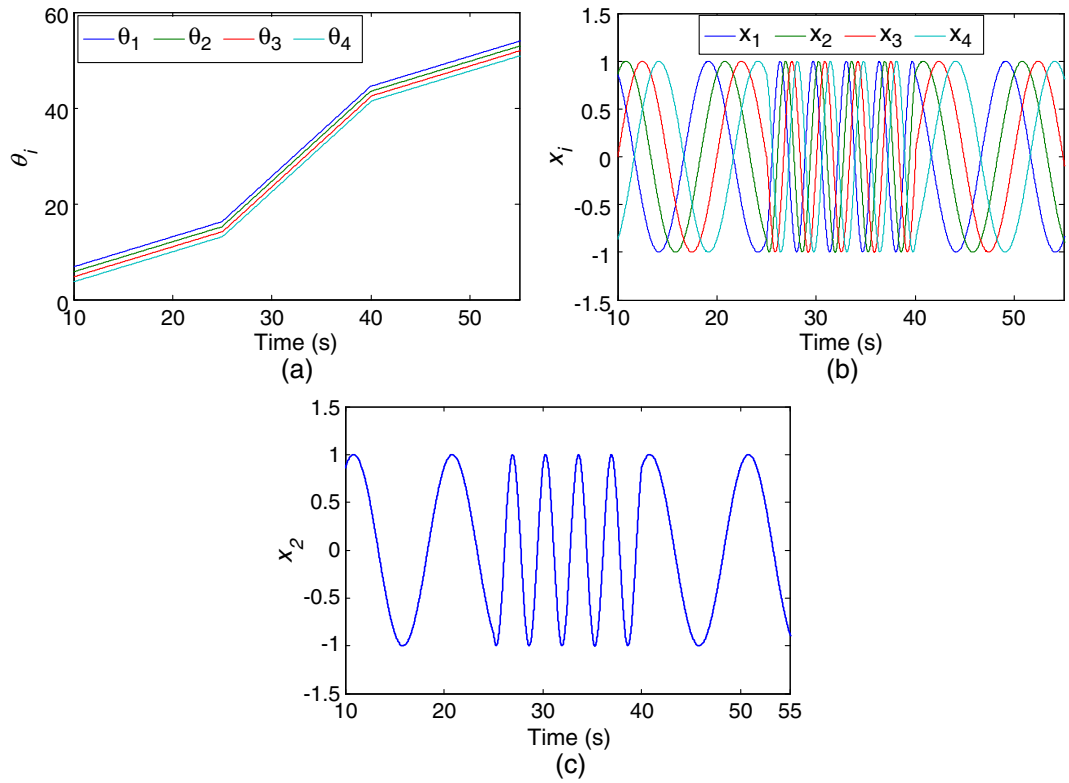

Fig. 10 Behavior of CPGs when changing τ at random time of 25 and 40 s: **a** θ_i with respect to time, **b** output x_i, **c** example of output of one CPG

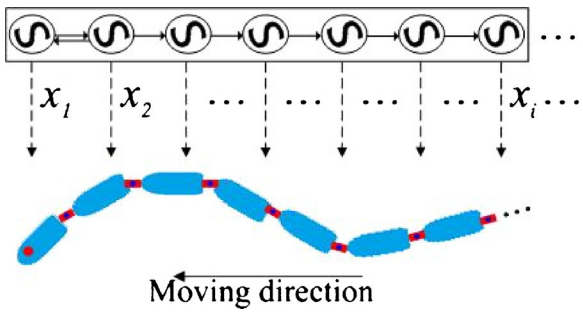

Fig. 11 CPG network implemented to control snake-like robot

from the interaction of the robot with the ground by swinging the joints from side to side [4]. Therefore, it is crucial to control the joint angle with constant phase difference.

4.1 Number of S-shape

Using the proposed structure of unidirectional coupling in Fig. 2b, the total phase difference, ϕ_{total} is given as follows:

$$\phi_{\text{total}} = n\phi \tag{20}$$

where n is the number of actuated joints from head to tail of the snake-like robot. To get one S-shape locomotion, the total phase difference should be equal to 2π. This is because, the CPG output of each of the joint actuator of the snake-like robot is in sequence with time at constant phase difference. Thus, the number of S-shape of the snake-like robot locomotion can be given as:

$$N = n\phi/2\pi \tag{21}$$

By changing the value of ϕ, we can obtain the desired serpentine locomotion of the snake-like robot, where Eq. 21 can be rearranged as follows:

$$\phi = 2\pi N/n \tag{22}$$

Hence, using Eq. 22, we can control the number of S-shape of the serpentine locomotion. Note that, the calculation of number of S-shape is the same for both unidirectional and bidirectional couplings.

Table 4 Physical parameters of simulated snake robot

Items	Details
Snake unit	$S_u = 6$
Length of snake unit [m^3]	$0.05 \times 0.08 \times 0.14$
Weight of snake unit	$w = 0.1$ kg
Radius of wheel	$r_w = 0.06$ m
Thick of wheel	$t_w = 0.015$ m
Weight of wheel	$w_w = 0.01$ kg
Friction coefficient	$\mu_N = 0.5$; $\mu_T = 0.01$

5 Simulation Results

Simulation of a snake-like robot has been conducted to verify the proposed CPG-based control method using open dynamic environment (ODE). Physical features of the snake-like robot are listed in Table 4 where two passive wheels are adopted to realize the swinging movement from side to side with ground asymmetric friction where the normal friction coefficient μ_N is larger than the tangential friction coefficient μ_T. Each of the snake unit is connected with joint actuator to drive the snake locomotion.

Figure 12 shows the simulation platform for the snake-like robot. The color of the head of the snake-like robot is different from other snake unit to differentiate between the first unit (head) and the last unit (tail) of the snake-like robot.

5.1 Control of Number of S-shape

The simulation results of the number of S-shape of the snake-like robot are shown in Fig. 13. Based

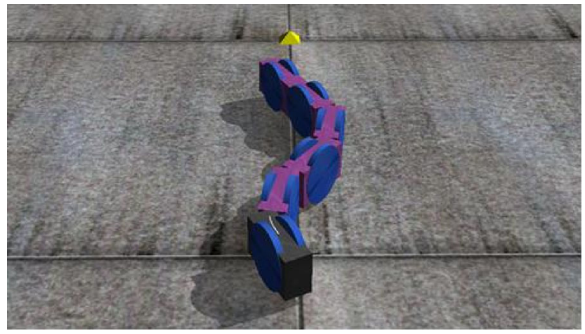

Fig. 12 Simulation platform of a snake-like robot

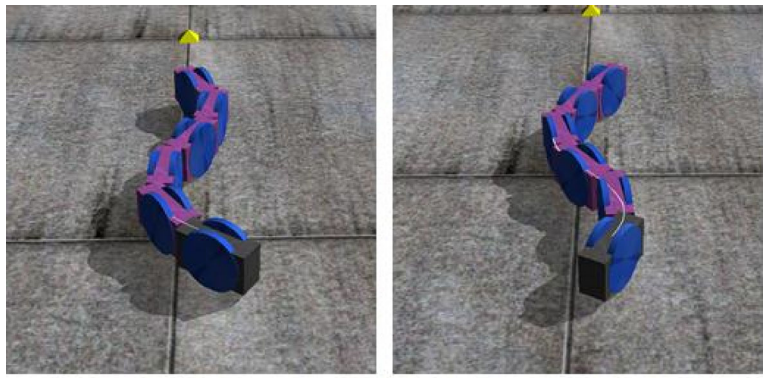

Fig. 13 Different number of S-shape obtain by simulation **a** $\phi = 8\pi/25$ ($N = 0.8$), **b** $\phi = 2\pi/5$ ($N = 1$)

on Eq. 22, we change the value of ϕ, to obtain different number of S-shape. For instance, with number of actuated joint, $n = 5$ (equal to $s_u - 1$), we can obtain desired number of S-shape by plugging different value of N. In our analysis, we used $N = 0.8$, and 1, where the value of $\phi = 8\pi/25$, and $2\pi/5$ respectively. Note that, the maximum or minimum number of S-shape is strictly depended on the physical features of the snake-like robot. Due to the limited numbers of the robot link, there will be a restriction in the number of S-shape that the snake-like robot can perform. In our case, the largest number of S-shape is $N = 1$. Thus, controlling the number of S-shape is one of the important criteria for the snake robot.

5.2 Forward and Backward Movement

Based on our analysis of the feedback connection of the CPGs, by changing the sign of ϕ of the first oscillator, we can change the output sequence of the CPGs. With that, using ODE simulation, we further analyze what is the effect to the locomotion of the snake-like robot. Since the CPGs output will be in reverse direction when we change the sign of ϕ, we then can control the movement direction the snake-like robot, as shown in Fig. 14.

The wave line in Fig. 14 is the head trajectory of the snake-like robot at the center of mass of the snake head. In Fig. 14a, all the other units of the snake-like robot are following the head trajectory

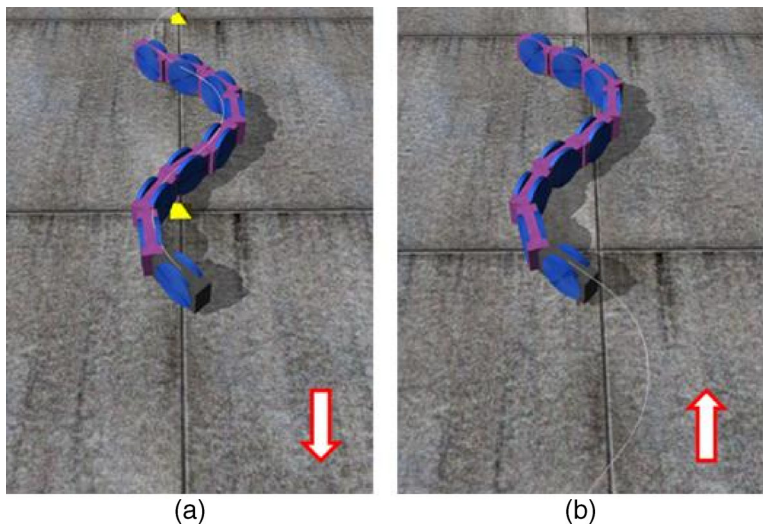

Fig. 14 Movement of a snake-like robot by simulation **a** forward movement **b** backward movement

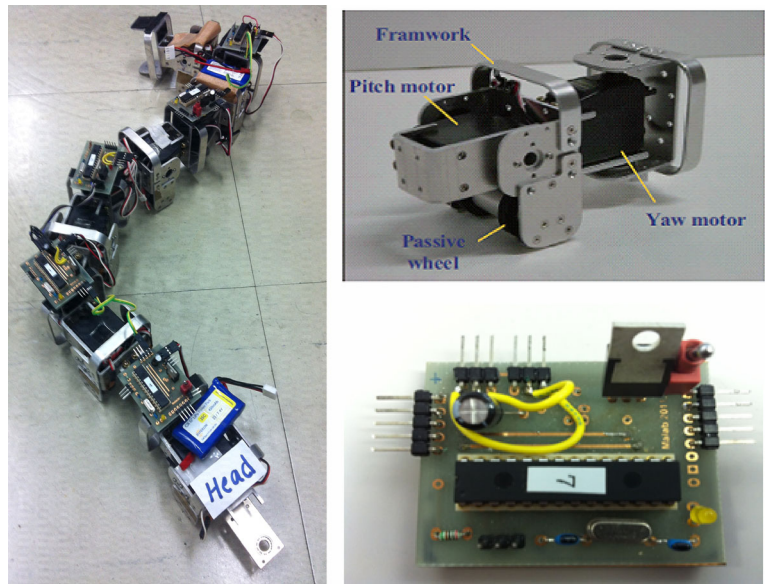

Fig. 15 Snake-like robot for experimental analysis

with forward motion. In Fig. 14b, the head trajectory line is at the back of the snake-like robot because of the backward movement. Therefore, the other snake units will not follow the head trajectory line. With this advantage, we can easily control the forward and backward movement of our snake-like robot just by changing the sign of the parameter ϕ.

6 Experimental Analysis

In this section, we will verify our proposed locomotion control into our snake-like robot. Figure 15 shows the image of our snake-like robot and its physical properties are described in Table 5. Note that, we can increase or decrease our snake unit depending on our objective. For this experiments, we will use only 6 units to verify our CPG model. In future, we will add more number of snake units for larger mobility.

For the experiment, each joint of the snake-like robot is controlled by one microcontroller unit (MCU) where each MCU corresponds to the CPG output, x_i. The CPG parameters used in this experiment are as follows: $\nu = 0.1$, $A = 1$, $w_{ij} = 10$, and $\tau = 1$.

6.1 Control of Number of S-shape

To verify the number of S-shape, we can observe locomotion curvature of the snake-like robot. The higher the number of S-shape, N the locomotion curvature will be smaller. For instance, in Fig. 16, we show different number of S-shape for $\phi = 8\pi/25$ ($N = 0.8$), and (b) $\phi = 2\pi/5$ ($N = 1$). For $N = 0.8$, we can observe that the locomotion curvature is asymmetric between the half body wave of the snake-like robot and the other half of the body wave. Meanwhile, for $N = 1$, the locomotion curvature is symmetric as one period of wave.

The number of S-shape can be controlled by manipulating the value of parameter ϕ using Eq. 22. The desired value of ϕ is inserted in Eq. 19 and the calculated CPG output, x_i with a gain inputs to the PWM to drive the joint motor.

Table 5 Description of the parameters

Items	Details
Snake unit	6
Size of each unit [mm^3]	$130 \times 62 \times 77$
Weight of each unit [kg]	0.28
Motion range of yaw angle [deg]	$[-90, +90]$
Actuator	RC servo motor

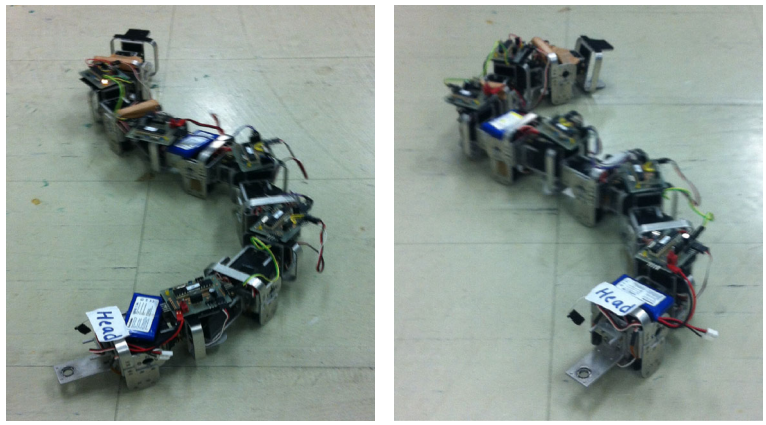

Fig. 16 Different number of S-shape obtain by experiment **a** $\phi = 8\pi/25$ ($N = 0.8$), **b** $\phi = 2\pi/5$ ($N = 1$)

6.2 Forward and Backward Movement

For forward and backward movement, the only change of the CPG parameters is the sign of the ϕ, where we can control the output sequence of the CPGs. Referring to Section 3.2, the sign ($\pm$) of ϕ for oscillator 1 should always be opposite to the other oscillators. For forward movement, the sign of ϕ for oscillator 1 is negative ($-$), which results in ascending order of the CPG outputs,

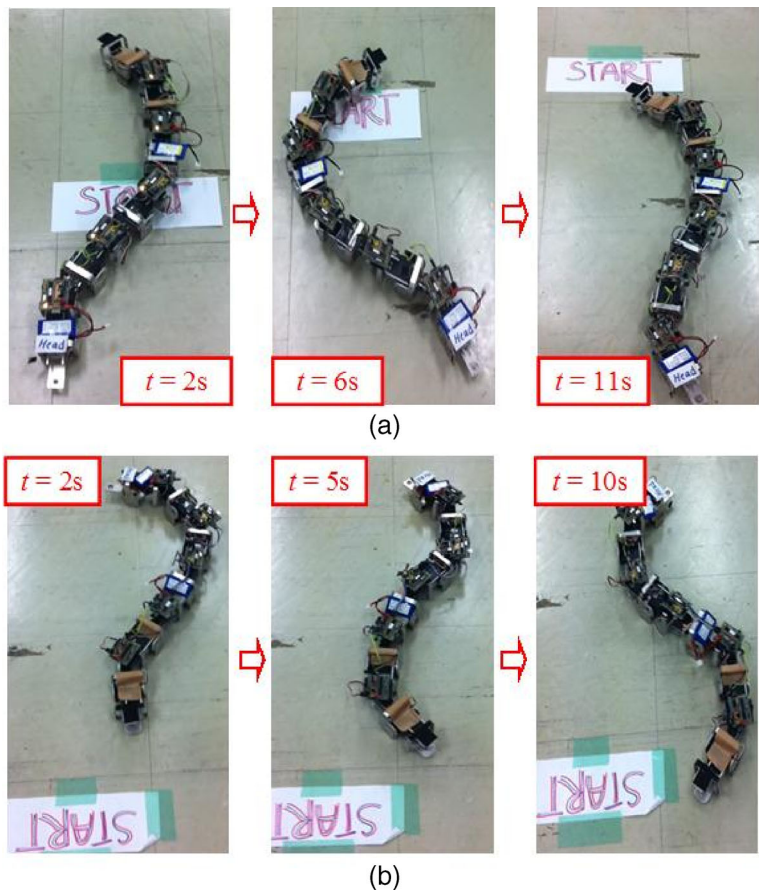

Fig. 17 Movement of a snake-like robot by experiment **a** forward movement **b** backward movement

whereas for backward movement, the sign of the ϕ is reversed. For the experimental verification, the setting of CPG parameters is similar as the simulation. Figure 17 shows the control of forward and backward movement of the snake-like robot by changing the the sign ($\pm$) of the parameter ϕ.

In Fig. 17, the difference between forward and backward movement of the snake-like robot is marked with the head of the snake-like robot and the direction of the written paper attached on the floor. Our experimental results verify the efficiency of our proposed CPG model.

7 Discussion

Based on the simulation and experiment results, we have verified the proposed unidirectional CPG structure can be used to control the locomotion of a snake-like robot. By changing parameter ϕ, we can control: (1) number of S-shape of the snake-like robot, and (2) forward and backward movement. However, the maximum number of S-shape should depend on the number of the snake-like robot link. The higher the link number, the higher number of S-shape can be performed. Also, there are specific procedures for the unidirectional CPG structure in order to realize the locomotion control of the snake-like robot as mentioned in Section 3.

Furthermore, we have compared our CPG structure with the bidirectional structure. With our proposed structure, we can achieve approximately the same convergence speed, less mathematical computation, and simplified structure. With just a mutual coupling between the first two CPGs, we can control our snake-like robot locomotion successfully with homogeneous distribution between the output of the oscillators. However, for a natural snake, it has the ability to perform assymmetric body shape during locomotion. We will investigate on how to mimic this characteristic based on our proposed CPG network.

During the experiments, each of the snake-like robot joint drives the motor according to the CPG output. To achieve higher locomotion efficiency, each of the joint motor should start simultaneously and this can be achieved by using a wireless module to send start signal to the head of the snake-like robot. Also, we have encountered a problem for the real time configuration of the snake-like motion. We know that by changing value of ϕ, we can change the S-shape of the snake-like robot. However, if we change ϕ instantly, the snake-like robot movement becomes harsh or jerky. This motion is not desired as it will damage the gear box or the motor. Therefore, in future, we will solve the problem by implementing activation function for smooth S-shape transition.

8 Conclusions and Future Works

In this paper, we have proposed an approach to design a CPG network with simplified structure to control the phase difference between coupled oscillators. Our proposed CPG network has been proven to have: (1) simple structure, (2) less computational cost, (3) fast convergence speed, and (4) converge to phase locking state. The phase difference can be used to control the serpentine locomotion using the phase oscillators as the CPG mathematical model. Additional parameter has been added to the phase oscillator to control the frequency and the smoothness of the CPG output simultaneously. With the proposed unidirectional network, the serpentine locomotion can be controlled by adjusting desired number of S-shape in one period.

In our future work, we will propose an approach to control locomotion of the snake-like robot to adapt to different space width by controlling the locomotion curvature. Also, we will investigate the adaptive control of amplitude of our CPG network without need to give any predefined value.

References

1. Wu, X.: CPG-based neural controller for serpentine locomotion of a snake-like robot. Doctoral dissertation, Science and Engineering, Ritsumeikan University (2011)
2. Ijspeert, A.J., Crespi, A.: Online trajectory generation in an amphibious snake robot using a lamprey-like

central pattern generator model. In: Proceedings of 2007 IEEE International Conference on Robotics and Automation, pp. 262–268. Roma, Italy (2007)
3. Nor, N.M., Ma, S.: A simplified CPGs network with phase oscillator model for locomotion control of snake-like robot. In: Proceedings of the 2012 IEEE International Conference on Robotics and Biomimetics, pp. 1299–1304. Guangzhou, China (2012)
4. Hirose, S.: Biologically Inspired Robot: Snake-like Locomotors and Manipulators. Oxford University (1993)
5. Lu, Z., Ma, S., Li, B., Wang, Y.: Serpentine locomotion of a snake-like robot controlled by musical theory. In: Proceeding of the 2005 IEEE/RSJ International Conference on Intelligent Robots and Systems, pp. 3019–3024. Edmonton, Canada (2005)
6. Zhou, C., Low, K.H.: Design and locomotion control of a biomimetic underwater vehicle with fin propulsion. IEEE/ASME Trans. Mechatron. **17**(1), 25–35 (2012)
7. Crespi, A., Ijspeert, A.J.: Online optimization of swimming and crawling in an amphibious snake robot. IEEE Trans. Robot. **24**(1), 75–87 (2008)
8. Lu, Z., Ma, S., Li, B., Wang, Y.: 3D locomotion of a snake-like robot controlled by cyclic inhibitory CPG model. In: Proceedings of the 2006 IEEE/RSJ International Conference on Intelligent Rrobots and Systems, pp. 3897–3902. Beijing, China (2006)
9. Wu, X., Ma, S.: CPG-based control of serpentine locomotion of a snake-like robot. In: Proceedings of the 9th International IFAC Symposium on Robot Control, pp. 871–876. Gifu, Japan (2009)
10. Tang, C., Ma, S.: A self-tuning multi-phase CPG enabling the snake robot to adapt to environments. In: Proceeding of the 2011 IEEE/RSJ International Conference on Intelligent Robots and Systems, pp. 1869–1874. San Francisco, USA (2011)
11. Collins, J., Richmond, S.: Hard-wired central pattern generators for quadrupedal locomotion. Biol. Cybernet. **71**, 375–385 (1994)
12. Chen, W., Ren, G., Zhang, J., Wang, J.: Smooth transition between different gaits of a hexapod robot via a central pattern generators algorithm. J. Intell. Robot. Syst. **67**, 255–270 (2012)
13. Taga, G.: A model of the neuro-musculo-skeletal system for anticipatory adjustment of human locomotion during obstacle avoidance. Biol. Cybernet. **78**(1), 9–17 (1998)
14. Williamson, M.M.: Rhythmic robot arm control using oscillators. In: Proceeding of the 1998 IEEE International Conference on Intelligent Robots and Systems, pp. 77–83. Victoria, Canada (1998)
15. Cohen, A.H., Holmes, P.J., Rand, R.H.: The nature of coupling between segmental oscillators of the lamprey spinal generator for locomotion: a mathematical model. J. Math. Biol. **13**, 345–369 (1982)
16. Olver, P.: Nonlinear ordinary differential equation. Online. Available at http://www.math.umn.edu/~olver/am_/odz.pdf
17. Sprowitz, A., Mockel, R., Maye, J., Asadpour, M., Ijspeert, A.J.: Adaptive locomotion control in modular robots. In: Workshop on Self-reconfigurable Robots Systems and Applications IROS, pp. 81–84 (2007)
18. Li, B., Li, Y., Rong, X.: Gait generation and transitions of quadraped robot based on Wilson–Cowan weakly neural networks. In: Proceedings of the 2010 International Conference on Robotics and Biomimetics, pp. 19–24. Tianjin, China (2010)
19. Liu, C., Chen, Q., Wang, D.: CPG-inspired workspace trajectory generation and adaptive locomotion control for quadraped robots. IEEE Trans. Syst Man Cybern. **41**(3), 867–880 (2011)
20. Anderson, G.T., Yang, Y., Cheng, G.: An adaptable oscillator-based controller for autonomous robots. J. Intell. Robot. Syst. **54**, 755–767 (2009)
21. Yu, J., Wang, M., Tan, M., Zhang, J.: Three-dimensional swimming. IEEE Robot. Autom. **18**(4), 47–58 (2011)
22. Inoue, K., Ma, S., Jin, C.: Neural oscillator network-based controller for meandering locomotion of snake-like robots. In: Proceedings of the 2004 IEEE International Conference on Robotics and Automation, pp. 5064–5069. New Orleans, LA (2004)
23. Matsuoka, K.: Sustained oscillations generated by mutually inhibiting neurons with adaptation. Biol. Cybern. **52**(6), 367–376 (1985)
24. Seo, K., Chung, S.J., Slotine, J.J.E.: CPG-based control of a turtle-like underwater vehicle. Auton. Robot **28**, 247–269 (2010)
25. Miller, G.: Neurotechnology for Biomimetic Robots. Chap. Snake Robots for Search and Rescue. MIT Press, Cambridge, MA (2002)
26. Prautsch, P., Mita, T.: Control and analysis of the gait of snake robots. In: Proceedings of the 1999 IEEE International Conference on Control Applications, pp. 502–507. Hawaii, USA (1999)
27. Lu, Z., Ma, S., Li, B., Wang, Y.: 3D locomotion of a snake-like robot controlled by cyclic inhibitory CPG model. In: Proceedings of the 2006 IEEE/RSJ International Conference on Intelligent Robots and Systems, pp. 3897–3902. Beijing, China (2006)
28. Ijspeert, A.J., Crespi, A., Ryczko, D., Cabelguen, J.M., From swimming to walking with a salamander robot driven by a spinal cord model. Science **315**(5817), 1416–1420 (2007)
29. Wu, X., Ma, S.: CPG-based control of serpentine locomotion of a snake-like robot. Mechatronics **20**(2), 326–334 (2010)
30. Ijspeert, A.J., Crespi, A., Cabelguen, J.M.: Simulation and robotics studies of salamander locomotion: applying neurobiological principles to the control of locomotion in robots. NeuroInformatics **3**(3), 171–196 (2005)